Naval Research Laboratory
Washington, DC 20375-5320

U.S. NAVAL RESEARCH LABORATORY

NRL/5340/MR—2021/7

A Procedure for Suppressing Multiple Scattering

MARGARET CHENEY

Colorado State University
Fort Collins, CO

MATTHEW J. BURFEINDT

Advanced Signal Processing Section
Radar Division

October 5, 2021

REPORT DOCUMENTATION PAGE

Form Approved
OMB No. 0704-0188

1. REPORT DATE *(DD-MM-YYYY)*	**2. REPORT TYPE**	**3. DATES COVERED** *(From - To)*
05-10-2021	NRL Memorandum Report	1 June 2021 – 10 August 2021

4. TITLE AND SUBTITLE

A Procedure for Suppressing Multiple Scattering

5a. CONTRACT NUMBER

5b. GRANT NUMBER

5c. PROGRAM ELEMENT NUMBER
61153N

6. AUTHOR(S)

Margaret Cheney*and Matthew J. Burfeindt

5d. PROJECT NUMBER

5e. TASK NUMBER

5f. WORK UNIT NUMBER
1L40

7. PERFORMING ORGANIZATION NAME(S) AND ADDRESS(ES)

Naval Research Laboratory
4555 Overlook Avenue, SW
Washington, DC 20375-5320

Colorado State University
Department of Mathematics
Louis R. Weber Building
841 Oval Drive, Fort Collins, CO, 80523

8. PERFORMING ORGANIZATION REPORT NUMBER

NRL/5340/MR--2021/7

9. SPONSORING / MONITORING AGENCY NAME(S) AND ADDRESS(ES)

Naval Research Laboratory
4555 Overlook Avenue, SW
Washington, DC 20375-5320

10. SPONSOR / MONITOR'S ACRONYM(S)

NRL Base Program

11. SPONSOR / MONITOR'S REPORT NUMBER(S)

12. DISTRIBUTION / AVAILABILITY STATEMENT

DISTRIBUTION STATEMENT A: Approved for public release; distribution is unlimited.

13. SUPPLEMENTARY NOTES

*Colorado State University, Department of Mathematics, Louis R. Weber Building, 841 Oval Drive, Fort Collins, CO, 80523

14. ABSTRACT

We introduce a method for removing multiple scattering components from radar signals by re-weighting the incident field. We first give the mathematical development of the technique. We then give several numerical examples. The examples demonstrate application of the technique to radar range profiles as well as synthetic aperture radar imagery.

15. SUBJECT TERMS

Radar
Born approximation
Multiple scattering
SAR

16. SECURITY CLASSIFICATION OF:			**17. LIMITATION OF ABSTRACT**	**18. NUMBER OF PAGES**	**19a. NAME OF RESPONSIBLE PERSON**
					Matthew Burfeindt
a. REPORT	**b. ABSTRACT**	**c. THIS PAGE**	U	20	**19b. TELEPHONE NUMBER** *(include area code)*
U	U	U			(202) 404-8696

Standard Form 298 (Rev. 8-98)
Prescribed by ANSI Std. Z39.18

This page intentionally left blank.

A Procedure for Suppressing Multiple Scattering

Margaret Cheney* and Matthew J. Burfeindt†

1 Introduction

Typical radar imaging methods such as synthetic-aperture radar rely on the Born or single-scattering approximation; this assumption, however, can result in image artifacts [3]. Consequently there is interest in developing radar imaging methods that avoid this assumption. But without the Born approximation, the radar imaging problem is nonlinear.

Some approaches to fully nonlinear multidimensional inverse problems have been developed in the math community. Examples are the d-bar method [11, 6] and the boundary control method [1, 12, 13]. The d-bar method applies to fixed-frequency data measured all around the boundary of an object. Numerical methods based on this method have been developed, and the approach is currently being used in electrical impedance tomography. However, it is difficult to see how to extend this method to the time-domain, limited-aperture data available in radar imaging. The boundary control method uses time-domain data, measured all around the boundary of an object; it is believed to be unstable. Very recently, a new "scattering control" method has been developed [4, 5], which proposes a method to modify the incident field in order to remove multiple scattering in the forward-propagating wave.

This document suggests a method to iteratively remove multiple scattering in a backscattered signal. This paper considers only the example of two ideal isotropic point-like scatterers, interrogated by a single antenna. The idea is to successively modify the incident field so the the field scattered from the closest scatterer cancels out the multiple scattering.

*Colorado State University
†US Naval Research Laboratory

Manuscript approved September 29, 2021.

This work is inspired by the work [14, 4, 5]. It does not quite fit into the scenario addressed in either paper. In particular [14] considers a purely one-dimensional case and uses an iterative modification of the incident field to produce an interior focus at a chosen location. The papers [4, 5], although they consider a fully three-dimensional case, control multiple scattering to a certain depth in the medium by iteratively modifying Cauchy data (the field and its time derivative) everywhere in a half-space.

This document considers a single antenna that can both transmit and receive signals.

2 Model for Multiple Scattering from Point Scatterers

Following [2, 9], we use the Foldy-Lax method [7, 8, 10, 16] plus the assumption [15] that the scattered field from a single "point" scatterer is proportional to the Green's function G. Here we assume that the isotropic point-like scatterers are located at positions $\boldsymbol{x}_1, \boldsymbol{x}_2, \ldots, \boldsymbol{x}_N$, and have scattering strengths $q_1, q_2, \ldots, q_N$. The Foldy-Lax method computes the multiple scattering from such separated scatterers by considering the "locally incident fields" $E^n, n = 1, 2, \ldots, N$ that are the incident fields seen by each scatterer at $\boldsymbol{x}_n$. The total scattered field is the sum of the scattered field from each scatterer:

$$E^{\text{sc}}(\boldsymbol{y}, \omega) = \sum_n G(\boldsymbol{y} - \boldsymbol{x}_n, \omega) q_n E^n(\boldsymbol{x}_n, \omega) \tag{1}$$

and each "locally incident field" E^n is the sum of the overall incident field E^{in} plus the fields scattered by all the other scatterers:

$$E^n(\boldsymbol{x}_n, \omega) = E^{\text{in}}(\boldsymbol{x}_n, \omega) + \sum_{m \neq n} G(\boldsymbol{x}_n - \boldsymbol{x}_m, \omega) q_m E^m(\boldsymbol{x}_m, \omega). \tag{2}$$

If the scattering strengths $q_1, q_2, \ldots, q_N$ are known, the system of linear equations (2) can be solved for the E^m; then the total field can be found from (1).

For the case $N = 2$, we write (2) in matrix form

$$\begin{pmatrix} 1 & -q_2 G(\boldsymbol{d}, \omega) \\ -q_1 G(\boldsymbol{d}, \omega) & 1 \end{pmatrix} \begin{pmatrix} E^1(\boldsymbol{x}_1, \omega) \\ E^2(\boldsymbol{x}_2, \omega) \end{pmatrix} = \begin{pmatrix} E_{\text{in}}(\boldsymbol{x}_1, \omega) \\ E_{\text{in}}(\boldsymbol{x}_2, \omega) \end{pmatrix}, \tag{3}$$

The solution to (2) is

$$\begin{aligned} E^1(\boldsymbol{x}_1,\omega) &= \frac{E_{\text{in}}(\boldsymbol{x}_1,\omega) + q_2 G(\boldsymbol{d}) E^{\text{in}}(\boldsymbol{x}_2,\omega)}{1 - q_1 q_2 G^2(\boldsymbol{d})} \\ &= \left(E^{\text{in}}(\boldsymbol{x}_1,\omega) + q_2 G(\boldsymbol{d}) E^{\text{in}}(\boldsymbol{x}_2,\omega)\right) \sum_{n=0} (q_1 q_2)^n G^{2n}(d) \\ E^2(\boldsymbol{x}_2,\omega) &= \frac{E^{\text{in}}(\boldsymbol{x}_2,\omega) + q_1 G(\boldsymbol{d}) E^{\text{in}}(\boldsymbol{x}_1,\omega)}{1 - q_1 q_2 G^2(\boldsymbol{d})} \\ &= \left(E^{\text{in}}(\boldsymbol{x}_2,\omega) + q_1 G(\boldsymbol{d}) E^{\text{in}}(\boldsymbol{x}_1,\omega)\right) \sum_{n=0} (q_1 q_2)^n G^{2n}(d) \end{aligned} \tag{4}$$

where $\boldsymbol{d} = \boldsymbol{x}_1 - \boldsymbol{x}_2$ and where for notational convenience we have suppressed the ω argument in G and have re-used the index n. We have also assumed that $|q_1 q_2 G^2(d)| < 1$ so that the expansion of the denominator as a geometric series is valid.

In (1) we substitute the locally incident fields (4) into (1). The scattered field is then

$$\begin{aligned} E^{\text{sc}}(\boldsymbol{y},\omega) = \Big[& G(\boldsymbol{y} - \boldsymbol{x}_1,\omega) q_1 \left[\left(E^{\text{in}}(\boldsymbol{x}_1,\omega) + q_2 G(\boldsymbol{d}) E^{\text{in}}(\boldsymbol{x}_2,\omega)\right)\right] \\ & + G(\boldsymbol{y} - \boldsymbol{x}_2,\omega) q_2 \left[\left(E^{\text{in}}(\boldsymbol{x}_2,\omega) + q_1 G(\boldsymbol{d}) E^{\text{in}}(\boldsymbol{x}_1,\omega)\right)\right] \Big] \sum_{n=0} (q_1 q_2)^n G^{2n}(d) \end{aligned} \tag{5}$$

Equation (5) expresses the overall scattered field at some observation point $\boldsymbol{y}$ as a sum of scattered fields from each scatterer. The terms in the sum over n correspond to multiple bounces back and forth between the scatterers.

3 Iterative Cancellation of Multiple Scattering

Here we consider the case of two point scatterers, with the multiple scattering modeled as above. We assume that the initial incident field is due to an isotropic antenna located at $\boldsymbol{y}$, so that

$$E^{\text{in}}(\boldsymbol{x},\omega) = F(\omega) \frac{e^{ik|\boldsymbol{x}-\boldsymbol{y}|}}{4\pi|\boldsymbol{x}-\boldsymbol{y}|}. \tag{6}$$

Then the scattered field at the antenna at $\boldsymbol{y}$ is $E^{sc} = SF$, where S is given by

$$S = S_0 \sum_{n=0}^{\infty} \left(q_1 q_2 \frac{e^{2ikd}}{(4\pi)^2 d^2} \right)^n \tag{7}$$

where S_0 is

$$S_0 = q_1 \frac{e^{2ikR_1}}{(4\pi R_1)^2} + q_2 \frac{e^{2ikR_2}}{(4\pi R_2)^2} + 2q_1 q_2 \frac{e^{ik(R_1+R_2+d)}}{(4\pi)^3 R_1 R_2 d} \tag{8}$$

and where $R_j = |\boldsymbol{y} - \boldsymbol{x}_j|$. When $F_0 \equiv 1$, which in the time domain corresponds to a sharp pulse at time $t = 0$, the scattered pulses have traveled distances $2R_1, 2R_2, R_1 + R_2 + d$, followed by the same list plus $2dn$, for $n = 1, 2, \ldots$. We assume $d < R_1 < R_2$, with $R_1 \approx R_2$.

The plan is to iteratively choose later pulses in the incident field F so that these later pulses cancel the multiple-scattering terms. Later pulses correspond to terms with larger phase. In (7), the earliest part of the field corresponds to the $n = 0$ term, and the direct scattering corresponds to the first two terms of (8).

This process could be carried out iteratively, with new incident waves being transmitted, or it could be carried out entirely within the computer after first measuring the scattering response to a time-domain broadband signal and Fourier transforming to obtain the scattering response S at each frequency.

3.1 Step 1

With $F_0 \equiv 1$, we denote the initial scattered field by $E_0^{sc} = SF_0$. We next look for $F_1 = F_0(1 + K_1)$ where K_1 is chosen so that when it scatters off the target at $\boldsymbol{x}_1$, its scattered field cancels the first multiple-scattering term:

$$K_1 q_1 \frac{e^{2ikR_1}}{(4\pi R_1)^2} + 2q_1 q_2 \frac{e^{ik(R_1+R_2+d)}}{(4\pi)^3 R_1 R_2 d} = 0 \tag{9}$$

We obtain

$$K_1 = -2q_2 R_1 \frac{e^{ik(R_2-R_1+d)}}{(4\pi) R_2 d} \tag{10}$$

In other words, K_1 is chosen to have a phase corresponding to the difference in arrival times between the first return and the first multiple-scattering return, and it is chosen to have an amplitude suitable for canceling the first multiple-scattering return.

We transmit F_1, and obtain the new scattered field $E_1^{sc} = SF_1 = S(F_0 + K_1)$. We note that the geometric series of (7) is common to all terms; consequently SF_1

is determined by the calculation

$$\begin{aligned} S_0F_1 = S_0F_0(1+K_1) &= F_0\left(q_1\frac{e^{2ikR_1}}{(4\pi R_1)^2} + q_2\frac{e^{2ikR_2}}{(4\pi R_2)^2} + 2q_1q_2\frac{e^{ik(R_1+R_2+d)}}{(4\pi)^3R_1R_2d}\right) \\ &\quad + F_0K_1\left(q_1\frac{e^{2ikR_1}}{(4\pi R_1)^2} + q_2\frac{e^{2ikR_2}}{(4\pi R_2)^2} + 2q_1q_2\frac{e^{ik(R_1+R_2+d)}}{(4\pi)^3R_1R_2d}\right) \\ &= F_0\left(q_1\frac{e^{2ikR_1}}{(4\pi R_1)^2} + q_2\frac{e^{2ikR_2}}{(4\pi R_2)^2}\right) \\ &\quad - 2F_0q_2R_1\frac{e^{ik(R_2-R_1+d)}}{(4\pi)R_2d}\left(q_2\frac{e^{2ikR_2}}{(4\pi R_2)^2} + 2q_1q_2\frac{e^{ik(R_1+R_2+d)}}{(4\pi)^3R_1R_2d}\right) \\ &= F_0\left(q_1\frac{e^{2ikR_1}}{(4\pi R_1)^2} + q_2\frac{e^{2ikR_2}}{(4\pi R_2)^2} - 2q_2^2R_1\frac{e^{ik(3R_2-R_1+d)}}{(4\pi)^3R_2^3d} - 4q_1q_2^2\frac{e^{ik(2R_2+2d)}}{(4\pi)^4R_2^2d^2}\right) \end{aligned} \tag{11}$$

which implies

$$\begin{aligned} E_1^{sc} = SF_1 = F_0&\left(q_1\frac{e^{2ikR_1}}{(4\pi R_1)^2} + q_2\frac{e^{2ikR_2}}{(4\pi R_2)^2} - 2q_2^2R_1\frac{e^{ik(3R_2-R_1+d)}}{(4\pi)^3R_2^3d} - 4q_1q_2^2\frac{e^{ik(2R_2+2d)}}{(4\pi)^4R_2^2d^2}\right) \\ &\times\sum_{n=0}^{\infty}\left(q_1q_2\frac{e^{2ikd}}{(4\pi)^2d^2}\right)^n \end{aligned} \tag{12}$$

The fourth term of the last line of (11) arrives at the same time as the field along the path that propagates from the antenna to $\boldsymbol{x}_2$, then from $\boldsymbol{x}_2$ to $\boldsymbol{x}_1$ and back to $\boldsymbol{x}_2$, and then returns to the antenna. This corresponds to one of the $n = 1$ paths in the sum in (7).

To summarize this first step, using an incident waveform $F_0(1 + K_1)$, where K_1 has phase $R_2 - R_1 + d$ and appropriate amplitude, we have converted the phases of E_0^{sc}, namely

$$(2R_1\ ,\ 2R_2\ ,\ R_1 + R_2 + d) + 2md(1,1,1), \qquad m = 0,1,2,\cdots \tag{13}$$

to those of E_1^{sc}, namely

$$(2R_1\ ,\ 2R_2\ ,\ 3R_2 - R_1 + d) + 2md(1,1,1), \qquad m = 0,1,2,\cdots. \tag{14}$$

Since $R_1 < R_2$, the new phase satisfies $3R_2 - R_1 + d = 2R_2 + (R_2 - R_1) + d > 2R_2 + d > R_1 + R_2 + d$. In other words, we have moved the initial multiple-scattering response to a later time.

Which occurs earlier, the new peak at $3R_2 - R_1 + d$ or the first triple-bounce peak, which occurs at $2R_1 + 2d$? We note that $3R_2 - R_1 + d = 2R_2 + R_2 - R_1 + d = 2R_1 + 2(R_2 - R_1) + R_2 - R_1 + d = 2R_1 + 3(R_2 - R_1) + d$; consequently when $3(R_2 - R_1) > d$, the new peak occurs later than $2R_1 + 2d$.

3.2 Step 2

We assume that $3(R_2 - R_1) < d$, so that the new peak at $3R_2 - R_1 + d$ arising from Step 1 is the next to be removed. We can repeat the process, finding $K_2 = |K_2|e^{ik\phi_2}$ whose phase ϕ_2 satisfies $2R_1 + \phi_2 = 3R_2 - R_1 + d$; in other words, $\phi_2 = 3R_2 - 3R_1 + d$. As above, the amplitude $|K_2|$ is chosen to cancel the initial multiple-scattering term of (12), which now has phase $3R_2 - R_1 + d$. In other words, K_2 should be chosen to satisfy

$$K_2 q_1 \frac{e^{2ikR_1}}{(4\pi R_1)^2} - 2q_2^2 R_1 \frac{e^{ik(3R_2 - R_1 + d)}}{(4\pi)^3 R_2^3 d} = 0 \tag{15}$$

or

$$K_2 = 2\frac{q_2^2}{q_1} R_1^3 \frac{e^{ik(3R_2 - 3R_1 + d)}}{(4\pi) R_2^3 d} \tag{16}$$

The scattered field for the waveform $F_0 K_2$ then contains terms whose phases are

$$(3R_2 - R_1 + d\ ,\ 5R_2 - 3R_1 + d\ ,\ 4R_2 - 2R_1 + 2d) + 2md(1,1,1). \tag{17}$$

The first phase can be used to cancel the desired one from (14). Here the third term involves triple-bounce scattering, and again appears later than the $n = 0$ terms of (13), but may not appear at the same time as other triple-bounce terms listed in (14).

The result of the scattering of the waveform $F_2 = F_0(1 + K_1 + K_2)$ is

$$\begin{aligned}
E_2^{sc} = SF_2 &= SF_1 + SF_0K_2 = E_1^{sc} + S_0K_2\sum_{n=0}^{\infty}\left(q_1q_2\frac{e^{2ikd}}{(4\pi)^2d^2}\right)^n \\
&= F_0\Bigg[q_1\frac{e^{2ikR_1}}{(4\pi R_1)^2} + q_2\frac{e^{2ikR_2}}{(4\pi R_2)^2} - 2q_2^2R_1\frac{e^{ik(3R_2-R_1+d)}}{(4\pi)^3R_2^3d} - 4q_1q_2^2\frac{e^{ik(2R_2+2d)}}{(4\pi)^4R_2^2d^2} \\
&\quad + \left(q_1\frac{e^{2ikR_1}}{(4\pi R_1)^2} + q_2\frac{e^{2ikR_2}}{(4\pi R_2)^2} + 2q_1q_2\frac{e^{ik(R_1+R_2+d)}}{(4\pi)^3R_1R_2d}\right)2\frac{q_2^2}{q_1}R_1^3\frac{e^{ik(3R_2-3R_1+d)}}{(4\pi)R_2^3d}\Bigg] \\
&\quad \times\sum_{n=0}^{\infty}\left(q_1q_2\frac{e^{2ikd}}{(4\pi)^2d^2}\right)^n \\
&= F_0\Bigg[q_1\frac{e^{2ikR_1}}{(4\pi R_1)^2} + q_2\frac{e^{2ikR_2}}{(4\pi R_2)^2} - 4q_1q_2^2\frac{e^{ik(2R_2+2d)}}{(4\pi)^4R_2^2d^2} \\
&\qquad + \frac{2q_2^3R_1^3}{q_1}\frac{e^{ik(5R_2-3R_1+d)}}{(4\pi)^3R_2^5d} + 4q_2^3R_1^2\frac{e^{ik(4R_2-2R_1+2d)}}{(4\pi)^4R_2^4d}\Bigg]\sum_{n=0}^{\infty}\left(q_1q_2\frac{e^{2ikd}}{(4\pi)^2d^2}\right)^n
\end{aligned} \tag{18}$$

Step 2 produces a new peak at $5R_2-3R_1+d$. To determine whether this is earlier or later than the first triple-bounce peak at $2R_1 + 2d$, we write $5R_2 - 3R_1 + d = 2R_1 + 5(R_2 - R_1) + d$. If $5(R_2 - R_1) > d$, this new peak occurs later than the first triple-bounce peak.

3.3 Step 3

We again assume that the new peak at $5R_2 - 3R_1 + d$ arising in Step 2 is the next one to be removed. Repeating the process above, we next find K_3 whose phase ϕ_3 satisfies $2R_1 + \phi_3 = 5R_2 - 3R_1 + d$; in other words, $\phi_3 = 5R_2 - 5R_1 + d$. The phases for F_0K_3 are

$$(5R_2 - 3R_1 + d\ ,\ 7R_2 - 5R_1 + d\ ,\ 6R_2 - 4R_1 + 2d) + 2md(1, 1, 1), \qquad m = 0, 1, 2, \cdots \tag{19}$$

Again the first phase can be used to cancel the desired one from (17), and the third involves triple-bounce scattering.

In particular, we choose K_3 to satisfy

$$K_3q_1\frac{e^{2ikR_1}}{(4\pi R_1)^2} + \frac{2q_2^3R_1^3}{q_1^2}\frac{e^{ik(5R_2-3R_1+d)}}{(4\pi)^3R_2^5d} = 0 \tag{20}$$

or

$$K_3 = -\frac{2q_2^3 R_1^5}{q_1^2}\frac{e^{ik(5R_2-5R_1+d)}}{(4\pi)R_2^5 d} \tag{21}$$

3.4 Step m

We see the pattern that the first multiple-scattering term is moved successively to $3R_2 - R_1 + d$, $5R_2 - 3R_1 + d$, $7R_2 - 5R_1 + d, \ldots$. The mth phase has the form $(2m+1)R_2 - (2m-1)R_1 + d = 2m(R_2 - R_1) + R_2 + R_1 + d$; as m increases, these correspond to later and later times.

We compare these new peaks to the first triple-bounce peak at $2R_1 + 2d$ by writing $(2m+1)R_2 - (2m-1)R_1 + d = 2R_1 + (2m+1)(R_2 - R_1) + d$. When $(2m+1)(R_2 - R_1) > d$, this new peak occurs later than the first triple-bounce peak, and the initial triple-bounce peak should be removed first.

3.5 Removing triple-bounce peaks

The first triple-bounce peak [involving the $n = 1$ term in the sum of (5)] occurs when the wave has traveled a distance of $2R_1 + 2d$. Thus, when this distance is smaller than those of peaks discussed previously, this one should be removed first. To remove it, we add to the transmitted waveform a contribution $F_0 H_1$ such that

$$H_1\frac{e^{2ikR_1}}{(4\pi R_1)^2} + \frac{e^{2ikR_1}}{(4\pi R_1)^2} q_1 q_2 \frac{e^{2ikd}}{(4\pi)^2 d^2} = 0 \tag{22}$$

or

$$H_1 = -q_1 q_2 \frac{e^{2ikd}}{(4\pi)^2 d^2} \tag{23}$$

Removal of the peak at $2R_2 + 2d$ appearing at the end of Step 2 can be done with an incident wave component $F_0 H_2$ such that

$$H_2 q_1 \frac{e^{2ikR_1}}{(4\pi R_1)^2} - 4q_1 q_2^2 \frac{e^{2ik(R_2+d)}}{(4\pi)^4 R_2^2 d^2} = 0 \tag{24}$$

or

$$H_2 = 4q_2^2 \left(\frac{R_1}{R_2}\right)^2 \frac{e^{2ik(R_2-R_1+d)}}{(4\pi)^2 d^2} \tag{25}$$

A similar procedure can be used to remove other terms.

4 Numerical Examples

Figure 1 shows the geometry for three numerical examples. The first example is a quasi-one-dimensional one in which only a single multipath return is visible; this simpler case illustrates the ideas more clearly. The second example is a fully three-dimensional one in which all multipath returns appear. The third is a synthetic aperture radar (SAR) imaging example. In the first two examples, the blue triangle in Fig. 1 marks the stationary location of the sensor. For the third example, the sensor is in motion in the y-direction and the blue triangle marks the center of the synthetic aperture.

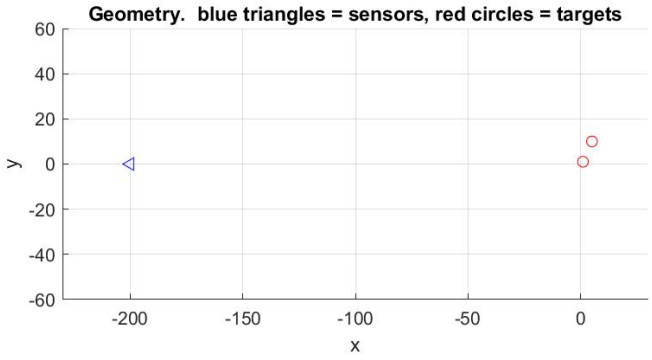

Figure 1: The sensor and target geometry.

4.1 One Round-Trip Bounce in Quasi-One Dimension

The initial example has the geometrical decay turned off to make the multipath easier to see. This means that this example is quasi-one-dimensional. A true one-dimensional example would require the wave to pass through the closest scatterer on its way to the distant one; but in these examples there is a direct path from the antenna to the more distant scatterer.

This initial example, moreover, shows only the direct scattering and only one round-trip multipath return. This makes the plots less cluttered and the underlying idea easier to see. Fig. 2 shows the original scattered waveform, and the results of the first four steps in pushing the multipath returns to later times. The peaks are

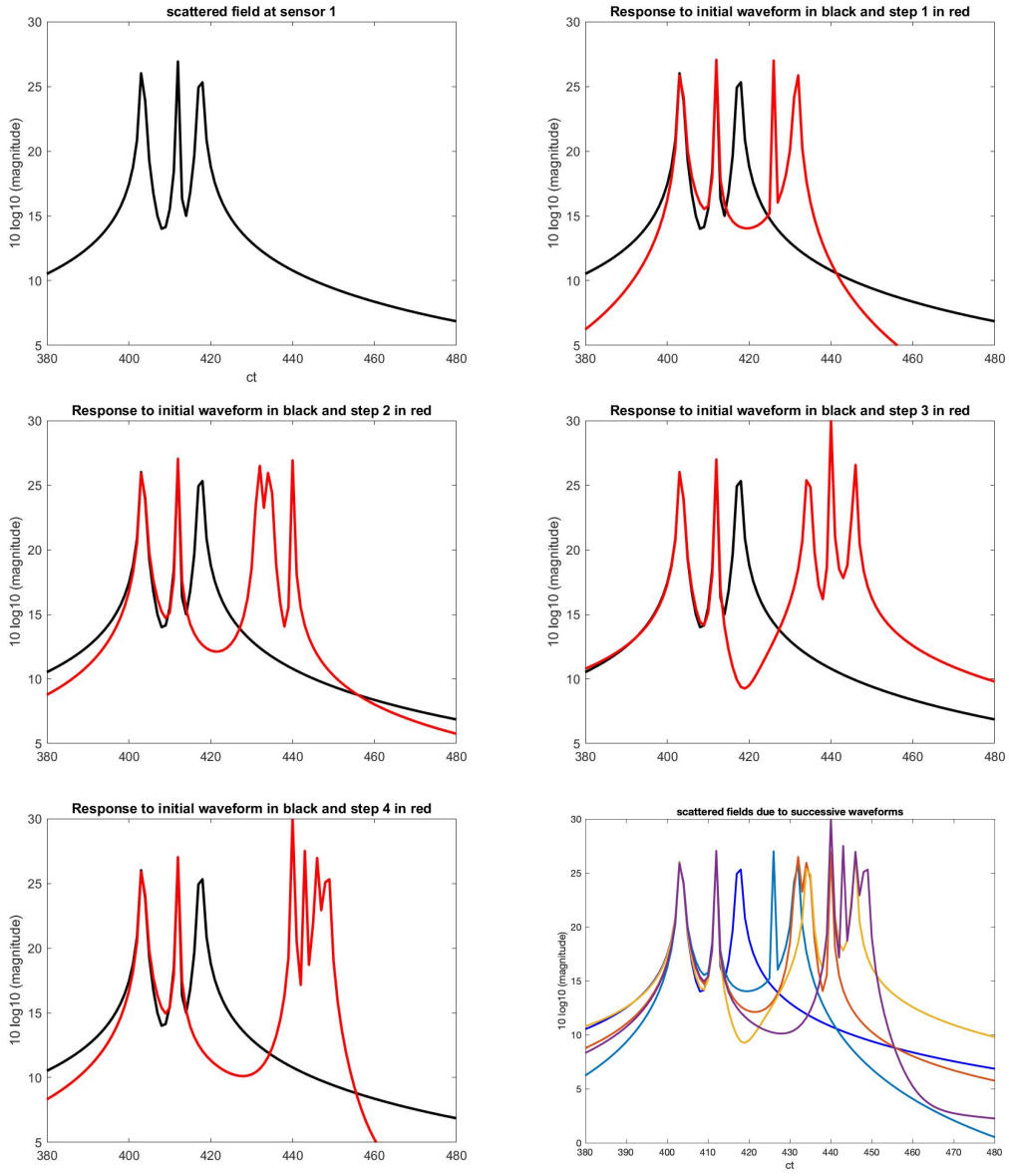

Figure 2: Scattering showing (top left) only one round-trip multipath return; (top right) the original return in black and the result of Step 1 in red; then (middle row) similar plots for the results of Steps 2 and 3; and (bottom left) a similar plot for the result of Step 4; (bottom right) all 4 returns on the same axes. Note that later plots show an increasingly wide gap where the initial third peak was located.

removed in chronological order, which is the order shown in Table 1. In particular, Step 3 removes the return at $2R_2 + 2d$, which above is described in the subsection on removal of triple-bounce returns.

Table 1: Approximate Peak Locations for $R_1 \approx 201, R_2 \approx 205, d \approx 10$

peak location formula	approx. value in simulation	notes
$R_1 + R_2 + d$	416	
$2R_1 + 2d$	421	not present in 1D example
$3R_2 - R_1 + d$	424	
$2R_2 + 2d$	430	
$5R_2 - 3R_1 + d$	433	

Fig. 3 shows the modified incident waveforms, each with one more spike than the previous one.

4.2 Multiple Bounces in Three Dimensions

This example shows multiple bounces [including the sum in (5)] in three dimensions. In other words, the geometrical decay is turned back on, and all the multipath returns are plotted, not just the first 3 returns as in the first example. This example uses $q_1 = q_2 = 40$ to make the multipath returns visible. Fig. 4 shows the original scattered return, and the results of the first four steps in pushing the multipath returns to later times. The peaks are removed in the order $R_1 + R_2 + d, 2R_1 + 2d, 3R_2 - R_1 + d$, and $2R_2 + 2d$.

Fig. 5 shows the modified incident waveforms, each with one more spike than the previous one.

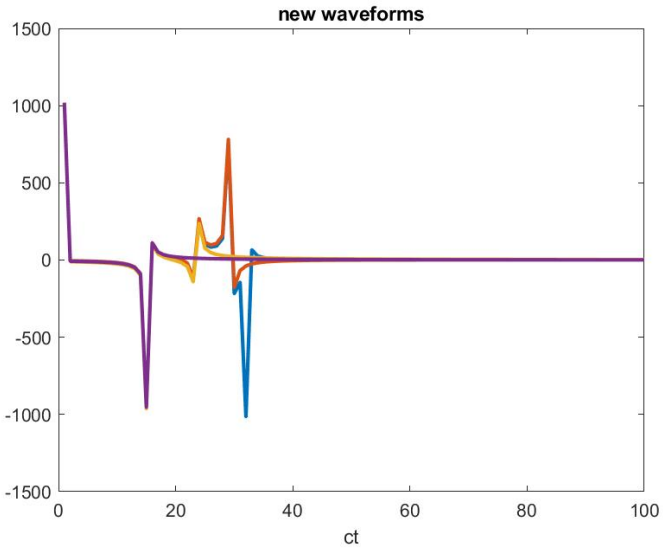

Figure 3: The modified incident waveforms. The time-domain version of F_1 is shown in purple; F_2 in yellow, and F_3 in red, and F_4 in blue. The early part of each waveform is the same as previous ones, but the later part adds an extra spike to cancel later-time responses.

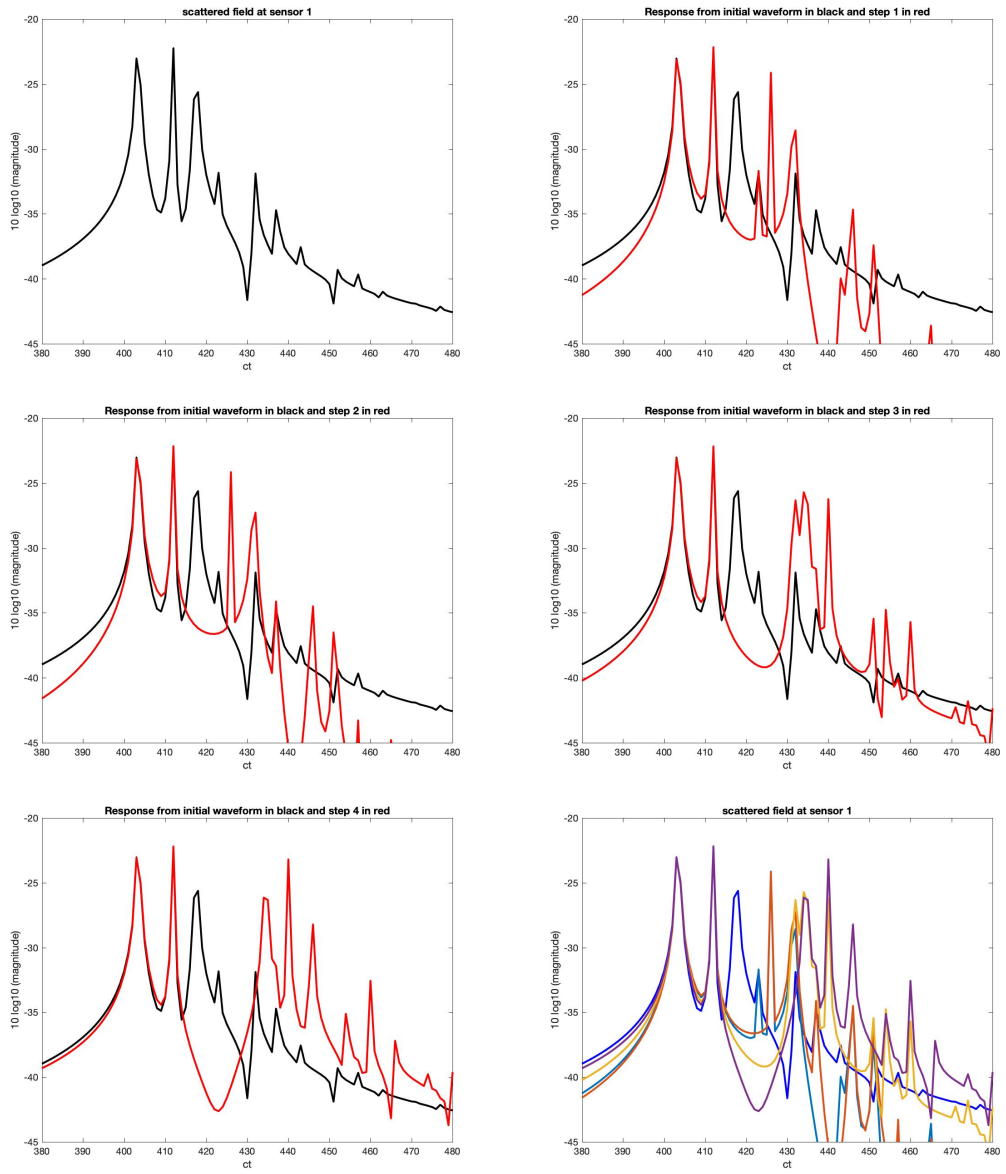

Figure 4: Scattering showing (top left) multipath returns in 3D; (top right) the original return in black and the result of Step 1 in red; (middle row) similar plots for the results of Steps 2 and 3; (bottom left) a similar plot showing the result of Step 4. The bottom right plot shows all 4 waveforms on the same axes. Note that later plots show an increasingly wide gap where the initial third, fourth, and fifth peaks were located.

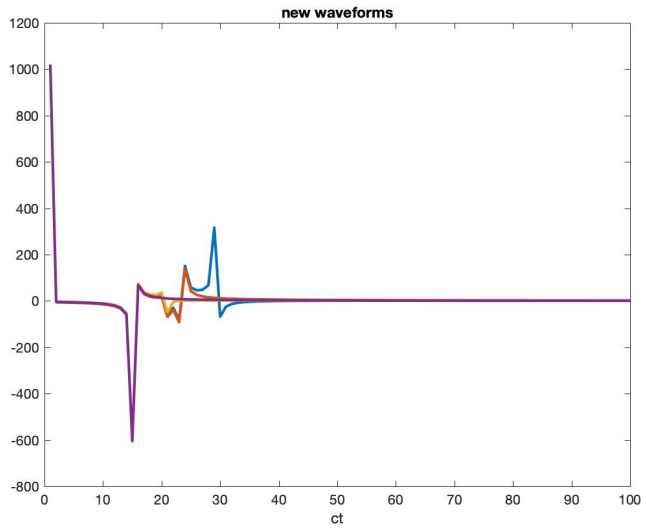

Figure 5: The modified incident waveforms. The time-domain version of F_1 is shown in purple, F_2 in yellow, F_3 in red, and F_4 in blue. The early part of each waveform is the same as previous ones, but the later part adds an extra spike to cancel later-time responses.

4.3 Radar Imaging

This example demonstrates the technique in a SAR imaging scenario. The sensor is moved in the y-direction across a synthetic aperture of length 30 m. The scattered signal is collected from $0.5 - 1.5$ GHz at 301 slow-time sample positions in the aperture. The scattering strengths are set to $q_1 = q_2 = 0.5$.

The scattering cancellation procedure is applied to SAR data in the following manner. For a given slow-time position, F_m is computed taking into account the dependence of R_1 and R_2 on the radar position in the synthetic aperture. The frequency-domain received signal for the slow-time position is then weighted by F_m. The procedure then repeats for all slow-time positions. In this way, the procedure can be applied in post-processing and does not require multiple passes if $m > 1$.

Hamming windows are then applied in fast- and slow-time to mitigate sidelobes. The SAR image is formed using the well-known backprojection algorithm. The results are shown for the first two steps in Fig. 6. As in the first example, only the first multibounce return is displayed for ease of demonstration. The results show that the multibounce return is pushed to higher range and cross-range positions with each step of the algorithm.

5 Iterative removal of scattering from second target

There seems to be no restriction that the removed peaks must correspond to multiple scattering. For example, the same procedure can be used to remove scattering from the target at $\boldsymbol{x}_2$. In this case, instead of choosing K_1 to satisfy (9), we choose the phase ϕ_1 to satisfy $2R_1 + \phi_1 = 2R_2$, so that $\phi_1 = 2(R_2 - R_1)$. Then, in the notation of (13), we have

$$(2R_2\ ,\ 4R_2 - 2R_1\ ,\ 3R_2 - R_1 + d) + 2md(1,1,1), \qquad m = 0, 1, 2, \cdots . \tag{26}$$

At the next stage we choose the phase ϕ_2 of K_2 to satisfy $2R_1 + \phi_2 = 4R_2 - 2R_1$, so that $\phi_2 = 4(R_2 - R_1)$ and the scattered phases are

$$(4R_2 - 2R_1\ ,\ 6R_2 - 4R_1\ , 5R_2 - 3R_1 + d) + 2md(1,1,1), \qquad m = 0, 1, 2, \cdots . \tag{27}$$

and so forth.

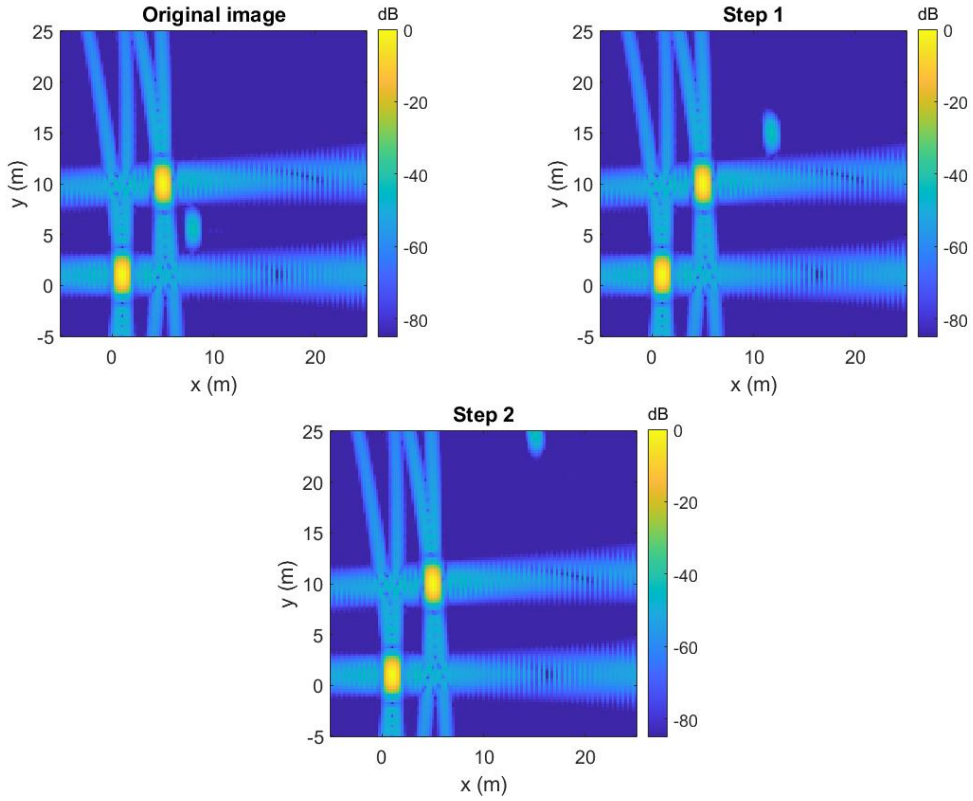

Figure 6: SAR results. (Top left) Image formed without using the scattering cancellation procedure, showing a single multibounce return. (Top right) Image formed using one step of the procedure. (Bottom) Image formed using two steps of the procedure. In all cases, 0 dB is referenced to the brightest pixel.

6 Discussion

This approach could potentially be used to remove scattering returns that obscure a nearby weaker return. The scattering centers of most realistic targets, however, are anisotropic and are unknown. We leave to future work the question of whether the peak locations and strengths can be determined with sufficient accuracy, without prior knowledge, to enable this "peak-pushing" approach to be useful.

7 Acknowledgment

M.C. thanks the ONR summer faculty program for supporting this work. She is also grateful to Matthew Burfeindt, Hatim Alqadah, and Dan Scholnik for hosting her virtual work at NRL.

References

[1] Belishev, Michael I. "Recent progress in the boundary control method." Inverse problems 23, no. 5 (2007): R1.

[2] M. Cheney and Borden, B. (2003). "Microlocal structure of inverse synthetic aperture radar data." *Inverse Problems,* 19(1), 173.

[3] M. Cheney and B. Borden (2009) *Fundamentals of Radar Imaging*, SIAM, Philadelphia.

[4] P. Caday, M. deHoop, V. Katsnelson, and G. Uhlmann, "Scattering control for the wave equation with unknown wave speed." Archive for Rational Mechanics and Analysis 231, no. 1 (2019): 409-464.

[5] P. Caday, M. deHoop, V. Katsnelson, and G. Uhlmann, "Reconstruction of piecewise smooth wave speeds using multiple scattering." Transactions of the American Mathematical Society 372, no. 2 (2019): 1213-1235.

[6] De Hoop, Maarten Valentijn, Matti Lassas, Matteo Santacesaria, Samuli Siltanen, and Janne P. Tamminen. "Positive-energy D-bar method for acoustic tomography: a computational study." Inverse problems 32, no. 2 (2016): 025003.

[7] A. J. Devaney, *Mathematical Foundations of Imaging, Tomography and Wavefield Inversion*. Cambridge University Press, 2012.

[8] L. L. Foldy, "The multiple scattering of waves: I general theory of isotropic scattering by randomly distributed scatterers," *Physical Review*, vol. 67, no. 3, pp. 107–119, February 1 1945.

[9] J.T. Kim, M. Cheney, and E. Mokole, "Tuning to resonances with iterative time reversal", IEEE Transactions on Antennas and Propagation 64.10 (2016): 4343-4354.

[10] Lax, Melvin. "Multiple scattering of waves." Reviews of Modern Physics 23, no. 4 (1951): 287.

[11] Mueller, Jennifer L., and Samuli Siltanen, *Linear and nonlinear inverse problems with practical applications*. Society for Industrial and Applied Mathematics, 2012.

[12] Oksanen, Lauri. "Solving an inverse obstacle problem for the wave equation by using the boundary control method." Inverse Problems 29, no. 3 (2013): 035004.

[13] Pestov, Leonid, Victoria Bolgova, and Oksana Kazarina. "Numerical recovering a density by BC-method." arXiv preprint arXiv:0906.0836 (2009).

[14] J.H. Rose, "Single-sided autofocusing of sound in layered materials." Inverse problems 18, no. 6 (2002): 1923.

[15] Snieder R K and Scales J A 1998 "Time-reversed imaging as a diagnostic of wave and particle chaos" *Phys. Rev. E* **58** 5668–75

[16] Tsang L, Kong J A and Shin R T 1985 *Theory of Microwave Remote Sensing* (New York: Wiley)